Nb-stabilized locally broken symmetry below and above T_c in a $PbZrO_3$ single crystal

D. Kajewski,* Z. Ujma, P. Zajdel, and K. Roleder
Institute of Physics, University of Silesia, ulica Uniwersytecka 4, 40-007 Katowice, Poland
(Received 19 November 2015; published 2 February 2016)

The influence of a small amount of niobium ions (0.6 mol% Nb_2O_5) introduced into $PbZrO_3$ single crystals on the structural, dielectric, optical, and electromechanical properties was studied. The main goal was to search for the influence of this doping on the phase transition sequence. It was found that addition of Nb leads to stabilization of the known intermediate phase and to formation of a new one. It is interesting that locally broken symmetry could be observed both below and far above the Curie temperature. All these results are analyzed in terms of charge compensation phenomena.

DOI: 10.1103/PhysRevB.93.054104

I. INTRODUCTION

Lead zirconate, $PbZrO_3$, has been of interest for dozens of years since its discovery [1–5]. Although its antiferroelectric character is not questioned, many reports still deal with the so-called intermediate phase, which appears in the range of a few degrees below the temperature of the transition to the paraelectric phase [6–11]. In spite of numerous experimental data, its origin and properties are not definitely known yet. Recently, through Brillouin light scattering, it was found that this phase can appear as a coexistence of the paraelectric and antiferroelectric phases rather than a phase of pure ferroelectric properties [7]. However, it is well known that deficiencies in Pb and O sublattices and dopants, especially Ti ions replacing Zr, stabilize the existence of this intermediate phase and make the temperature range of its existence much wider [12–21].

Relatively fewer data are available in the literature concerning the influence on lead zirconate properties of nonisovalent dopants such as Nb^{5+} [22–25]. In fact, it was Benguigui [22] who first wrote a paper [22] dealing with this issue. To some degree in this paper we come back to his idea and thus expect that Nb dopants may lead—in $PbZrO_3$—to defects in the charge neutrality of the crystal lattice during the growth process, especially in the Pb or O sublattices as already mentioned. We also guess that due to the radius of Nb ions they most likely would occupy the center of oxygen octahedra.

The aim of this work was, thus, to investigate the influence of a small amount of Nb on the structural, optical, dielectric, and electromechanical properties of a single $PbZrO_3$ crystal, and thus to characterize the structural transformations which this Nb-doped crystal undergoes.

II. EXPERIMENTAL CONDITIONS

Lead zirconate single crystals, doped with a nominal Nb_2O_5 concentration of 0.6 mol% were grown from high-temperature solutions, by means of spontaneous crystallization (flux growth method). The starting raw materials PbO, PbF_2, B_2O_3, and $PbZrO_3$:0.6 mol% Nb_2O_5 in the form of ceramics were weighed and mixed together (the ceramic preparation was already described elsewhere [23]).

A one-zone resistance furnace was controlled with a microprocessor temperature regulator. The mixture was melted and synthesized in a Pt crucible. The crucible, covered with a Pt lid, was heated up to 1300 K. The temperature, measured under the bottom of the crucible, was kept stable for at least 5 h to enable complete soaking of the melt. After soaking, the melt temperature was lowered at the rate of 2.5 K/h, down to 1150 K. In the next step the remaining melt was decanted and the as-grown crystals attached to the crucible walls were cooled to room temperature at the rate of 10 K/h. In the final step, the crystals were etched in diluted acetic acid to remove residues of solidified flux. The obtained crystals were of red color and optically transparent. The stoichiometry of the crystals obtained was checked by means of a RIGAKU ZSX Primus II x-ray fluorescence spectrometer (XRF). Powder diffraction measurement was carried out on a PANalytical PW1050 diffractometer, using a nickel-filtered Cu $K\alpha_{1,2}$ source, operating at 30 kV/30 mA. A 15 mg crystal was ground in an agate mortar and deposited on double-sided Scotch tape attached to a glass slide. The diffractogram was collected in a step mode, with 0.02 ° step in the angular range of 7 °–135 °. The beam spilled over the sample under 17 °, which was later corrected in the refinement. The instrument resolution file was obtained from an internal silicon standard ($a = 5.431\,194$ Å). The Rietveld refinement [26] was carried out using the FULLPROF software suite [27].

The birefringence measurements were performed by means of an Oxford Cryosystems Metripol birefringence imaging system (Metripol [7]). The sample was held in a high-precision Linkam TMSG600 temperature stage combined with the Metripol system. A detailed description of this automated optical technique can be found in the paper by Geday and Glazer [28]. The measurement method for the piezoelectric and electrostrictive strain has been reported by Wieczorek *et al.* [29].

An automated measuring system with HP 4192A impedance analyzer was used to measure the capacity C and conductance G in parallel circuit mode. Prior to measurements, silver paste electrodes were attached to the samples andthey were rejuvenated at 390 °C for 10 min.

III. CHEMICAL AND STRUCTURAL ANALYSIS

It is not an easy task to estimate the Nb content in the volume of lead-based compounds. This is because both ions

*Corresponding author: dariusz.kajewski@us.edu.pl

reveal x-ray spectra that overlap in energy-dispersive x-ray spectroscopy (EDS). We have thus tried to use chemical analysis by means of x-ray fluorescence spectrometry, which has revealed a ca. 0.5 mass% lead excess in comparison with the theoretical value. This could be explained by the lead-rich flux used for the crystal growth process, in order to prevent lead vacancy creation at high temperature. However, taking into account the sensitivity and features of the XRF method, this lead excess has to be imputed rather to a thin surface layer of the order of tens of nanometers than to crystal volume. For the same reason, it was also possible to determine the niobium concentration. Investigations revealed a much smaller concentration of niobium than the nominal one. Only 0.13 mass% of Nb was introduced, instead of 0.42 mass%, which is equal to the nominal 0.6 mol% of Nb_2O_5. It is well known that elements with 5+ oxidation states used as dopants are difficult to introduce into perovskite lattices. This is because of the charge compensation needed to get lattice electrical neutrality. Thus, we describe the crystal obtained using the nominal 0.6 mol% concentration of Nb_2O_5 in the flux.

Based on what has been said above, the most probable situation is substitution of Nb ions for Zr [22,23]. This may lead to four possible situations:

(1) Niobium changes its oxidation state to Nb^{4+}, giving one electron to the conduction band.

(2) Niobium situates itself next to a lead vacancy, i.e., two niobium ions are necessary to compensate the charged Pb^{2+} vacancy to keep electrical neutrality.

(3) Two niobium atoms create one Pb^{2+} lead vacancy.

(4) One should also consider that the oxides used for synthesis could possess some acceptor impurities such as K or Na, creating charged oxygen vacancies. In such cases two Nb ions will compensate one oxygen vacancy.

A starting model in the orthorhombic *Pbam* space group was used, based on a structure published by Yamasaki *et al.* [30]. The line shape was modeled using the Thompson-Cox-Hastings [31] approach with anisotropic strain [32] and size [33] broadening implemented in FULLPROF. The x-ray pattern of $PbZrO_3$:Nb obtained at room temperature is presented in Fig. 1. The refined parameters included three lattice parameters, anisotropic atomic displacement (ADP) parameters for Pb1, Pb2, Zr, and one common ADP for all of the oxygen sites, three size and three strain coefficients, and an asymmetry factor. The background was modeled using linear interpolation between 18 points of refinable heights. A further refinement revealed an evident preferred orientation (PO) problem, as two families of (120) and (002) reflections were stronger for the diffraction pattern. Unfortunately, any modeling of the PO using models built into the FULLPROF suite did not improve the fit, so three angular regions (21.00, 22.00), (43.00, 44.30), (72.30, 73.00), containing the strongest PO peaks were removed from the refinement. All reflections were indexed within the *Pbam* space group and no additional peaks were observed, confirming the symmetry chosen. The low values of the parameters (in %): $R_p = 3.73$, $R_{wp} = 4.83$, $R_{exp} = 3.04$, $R_{Bragg} = 4.62$, RF = 7.93, and $\chi^2 = 2.53$, indicate good refinement, with the restriction that oxygen positions are usually not very well resolved from x-ray diffraction. The unit cell parameters were found to be $a = 5.8806(1)$ Å, $b = 11.7797(2)$ Å, and $c = 8.2251(1)$ Å (the reported errors are statistical on the 1σ level). In comparison with $a = 5.888\,42$ Å, $b = 11.771\,40$ Å, and $c = 8.226\,30$ Å for undoped $PbZrO_3$ crystals, the b parameters increased slightly [30,34]. This leads to a decrease in unit cell volume from 570.206 $Å^3$ for pure $PbZrO_3$ to 569.61 $Å^3$ for the $PbZrO_3$:Nb crystal.

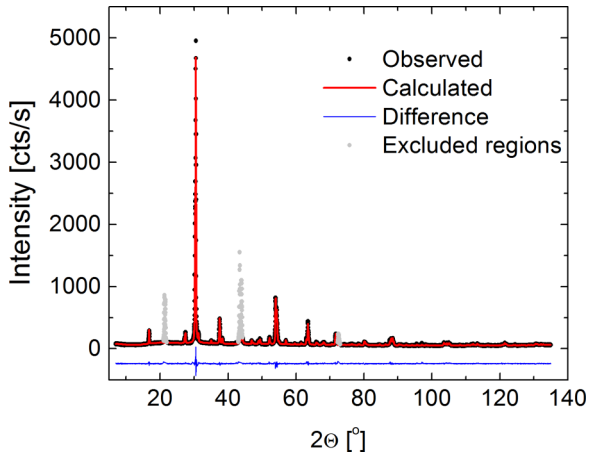

FIG. 1. Diffraction pattern of $PbZrO_3$:Nb at room temperature.

Because the ionic radius of Nb^{5+} is much smaller than the radius of lead, it is unlikely that niobium ions substitute for Pb^{2+}. Thus, the preferred position to be occupied by Nb is that of Zr ions, so this could explain the decrease in unit cell volume.

IV. DIELECTRIC MEASURMENTS

The same crystal was used in measurements of capacitance C and conductance G, from which the permittivity ε' and dielectric losses $\tan\delta$ were ascertained. Examples of $\varepsilon'(T)$ runs at a measuring field of 0.01 kV/cm and frequency of 800 kHz are presented in Fig. 2.

One can observe two significant anomalies: the first above 230 °C and the other near 221 °C and 225 °C, respectively, for cooling and heating [Fig. 2(a)]. Careful analysis of the dielectric permittivity revealed the existence of another diffuse anomaly [see the arrows in Fig. 2(b)]. This suggests that an additional phase transition has evolved in the single crystal, which has apparently not been observed in ceramic samples [23]. Thus here two intermediate phases below T_C are observed in niobium-doped lead zirconate.

An exemplary plot of $\varepsilon'(T)$ on cooling is presented in Fig. 3. It is easy to notice that much above T_C the Curie-Weiss law is not obtained. This could be explained by the existence of stable or thermally fluctuating noncentrosymmetric micro/nano-regions, the nature of which has been earlier reported in a paper on pure lead zirconate [35]. Such nanoregions (nanoclusters) should be treated simply as a noncentrosymmetric local structure embedded into a centrosymmetric matrix. Thus, a specific coexistence of two phases above T_C should be taken into account, also in the case of $PbZrO_3$:Nb single crystals.

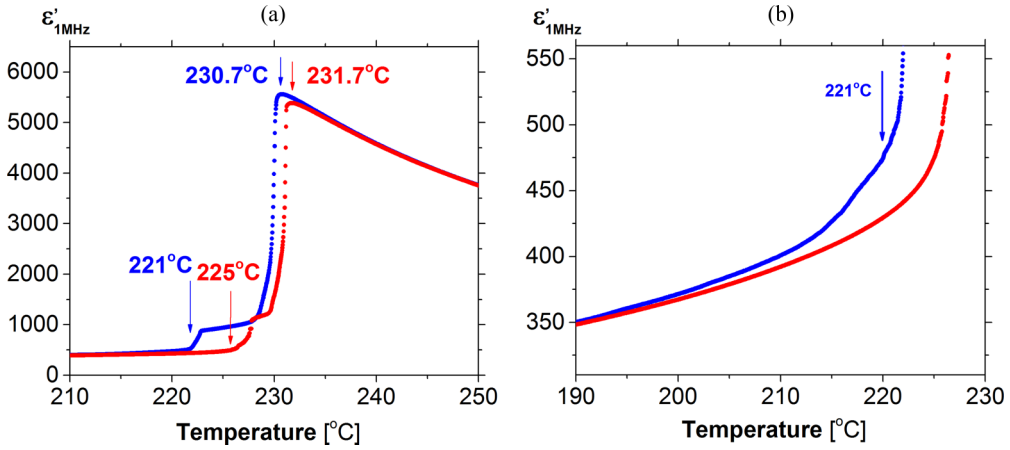

FIG. 2. (a) Real part of permittivity ε vs temperature for $PbZrO_3$:Nb crystal, for heating and cooling (1 K/min). (b) The arrow indicates another anomaly of ε' on cooling for the $PbZrO_3$:Nb crystal, not observed in ceramics of the same chemical composition. One can see clearly the disappearance of dielectric thermal hysteresis towards 200 °C.

The temperature region of such coexistence is better represented by a run of differences between reciprocal values of measured permittivity and values received by a fit to Curie-Weiss law, at higher temperatures (Fig. 4). It is interesting to distinguish the point T_{pd} in this figure. As described in Sec. VI, this is a temperature at which very clear piezoelectric deformations were observed. It means that T_{pd} is a limit up to which thermally and mechanically persistent noncentrosymmetric regions should be present. Otherwise, the presence of piezoelectric signals would not be justified. Above this temperature, where the pure Curie-Weiss law is still not fulfilled, one can speak about polar fluctuations, of the order of a few units at T_{BH}, which may lead to dynamically appearing and/or disappearing local polarity. Its chaotic/random orientation in space leads to a macroscopically centrosymmetric phase. Finally, as shown in Fig. 4, the *pure* paraelectric phase is realised much above 300 °C.

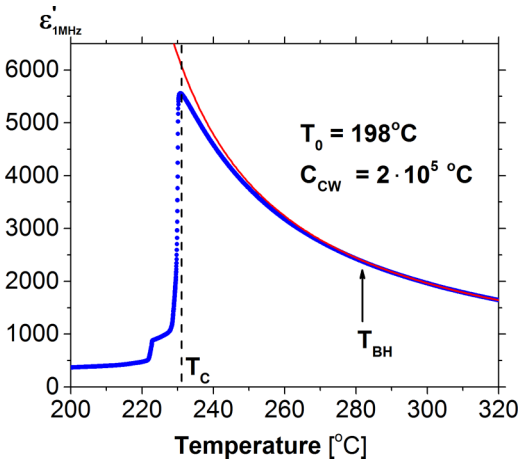

FIG. 3. Permittivity versus temperature for $PbZrO_3$:Nb crystals. The arrow indicates a point T_{BH}, below which the Curie-Weiss law (red line) is not obeyed. T_{BH} is the Bussmann-Holder temperature equal to $1.1T_C$. It represents a theoretical limit of noncentrosymmetric clusters that start growing rapidly on approaching T_C from the high-temperature side [7].

V. OPTICAL PROPERTIES

The Metripol setup mentioned in Sec. II introduces experimental data equivalent to planar birefringence maps of samples under investigation. Such maps, received under no other external fields but temperature only, give direct information about phase transitions points. Figure 5 represents arbitrarily chosen maps for phases in between transition points. The false color technique has allowed us to find out that inside the two intermediate phases, the irregular domain pattern with 180° and 90° domain boundaries is present. The colors represent the value of birefringence from low (pink color) to highest values (red color). However, the most interesting result is connected with Fig. 5(d). This birefringence map shows the structure of microdomains with irregular (rounded) boundaries and with rotated optical axes of indicatrices. Such structure, observed down to room temperature, may originate from clustering of niobium ions inside the antiferroelectric phase. Here, it is worth mentioning that the tendency of heterovalent Nb to create clusters in the perovskite structure has been reported by Rodenbücher *et al.* [36] for niobium-doped strontium titanate.

Recently we reported [7,37,38] that in oxide perovskites the phase above T_C, in a defined and quite wide temperature region, is birefringent. Also in the case of Nb-doped lead zirconate similar phenomena as those presented in Fig. 6 have been observed.

VI. ELECTROMECHANICAL PROPERTIES

Measurements of the piezoelectric coefficient d_{33} and electrostrictive strain were performed in a wide temperature range for heating and cooling. Temperature changes of the piezoelectric signals on cooling are presented in Fig. 7.

The maximum of the piezoelectric response is observed near the temperature at which ε_{max} appears. It is interesting that d_{33} is observed both above T_C and from T_C down to 205 °C, changing the character of the run close to 221 °C, which is the limit of the first intermediate phase existence. This means that this intermediate phase does not possess a center of symmetry under an ac electric field. We believe that the strongest and most irregular changes of the module d_{33} observed up to 221 °C

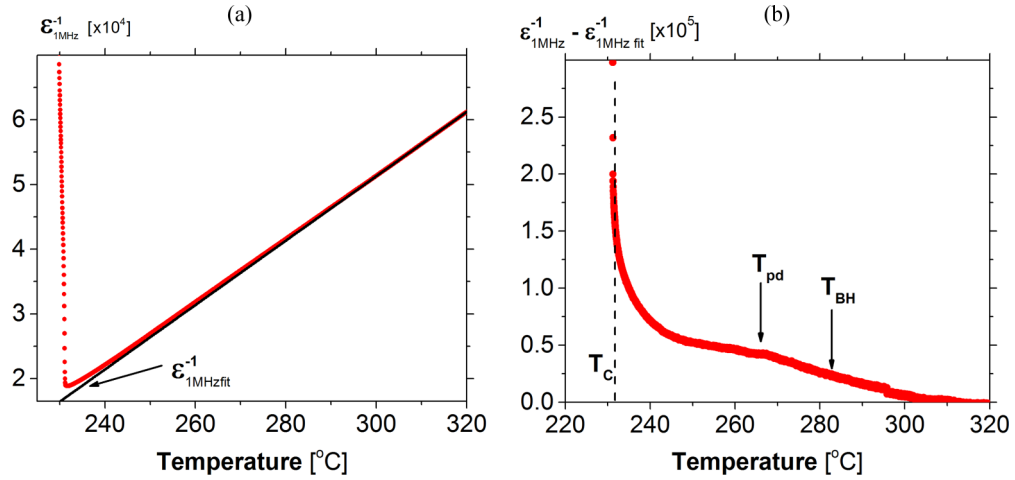

FIG. 4. (a) Reciprocal permittivity as a function of temperature above T_C. The black line is a fit to the Curie-Weiss law $C/(T - T_0)$. (b) The difference between reciprocal permittivity $\varepsilon^{-1}_{1\ \mathrm{MHz}}$ detected and fitted $\varepsilon^{-1}_{1\ \mathrm{MHz\ fit}}$ as a function of temperature. The point T_{pd} is the temperature at which piezoelectric signals disappear (see Fig. 6 further in the text), and—as in Fig. 3—T_{BH} is the Bussmann-Holder temperature. The difference in reciprocal permittivity becomes negligible at temperatures higher than T_{BH} because it reflects the existence of competing lattice instabilities at the Γ and R points, which are present at all temperatures above T_C [7], and to which the low-frequency permittivity is sensitive enough, even at 300 °C. Such dependence is observed on both cooling and heating.

are caused mainly by incomplete domain movements in an external electric field. In fact, complex domain structures, with 90° domain boundaries, have been observed during birefringence measurements [see Fig. 5(b)]. Going down with temperature, the piezoelectric response between 221 and 205 °C is weaker and almost monotonic, although complex domain structure is still present. This is the range in which the second intermediate phase evolves. To answer the question why the piezoelectric effect is weak in this phase, one may suppose that domains become strongly pinned. A proof of that is the map of birefringence in Fig. 5(c), showing clearly separated regions of domains oriented in the same direction. These are the strips of the same value of birefringence, i.e., the same color in Fig. 5(c), including noncentrosymmetric regions (the strip of the pink color), coexisting with the piezoelectric ones. Another proof that domains are strongly pinned in the range of the second intermediate phase is a lack of electrostrictive response below 205 °C (Fig. 8). It is because the electrostrictive response below T_C is mainly due to reorientations of domains in the alternating electric field.

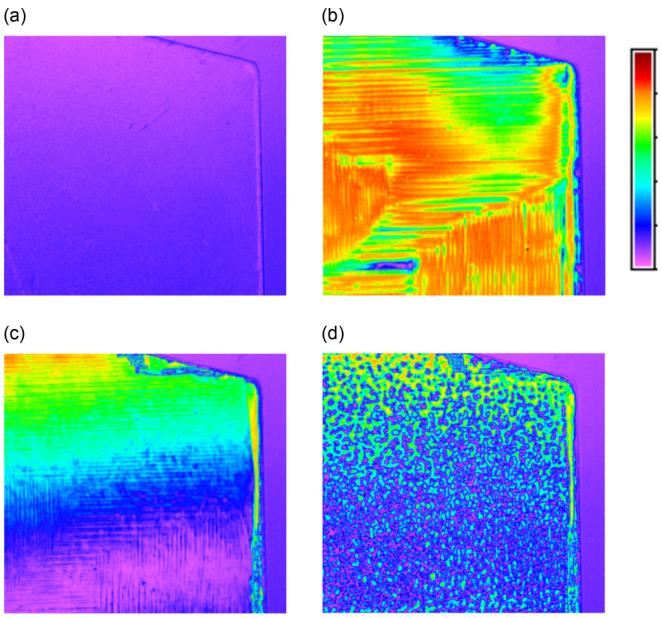

FIG. 5. Birefringence maps of a single $PbZrO_3$:Nb crystal registered on cooling: (a) above T_C, at 235 °C, (b) below T_C, within the first intermediate phase, at 229 °C, (c) within the second intermediate phase, at 215 °C, and (d) within the antiferroelectric phase, at 186 °C. The bar with gradient of colors represents values of birefringence from 0 (pink color) to nonzero values (the red color represents the highest value in a defined investigated region).

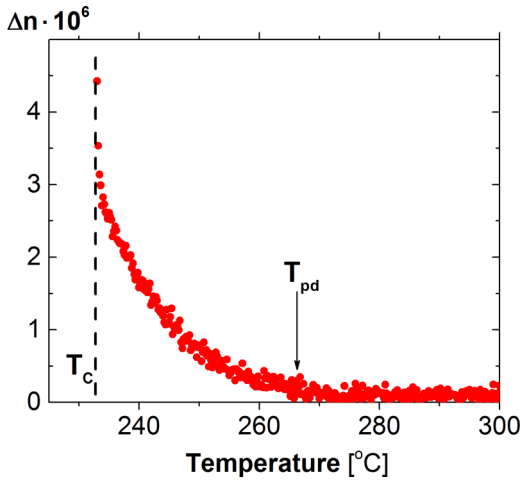

FIG. 6. Birefringence above T_C for a single $PbZrO_3$:Nb crystal. The nonzero birefringent phase has been evolving up to temperature T_{pd}, at which piezoelectric signals vanish (see Fig. 7 further in the text).

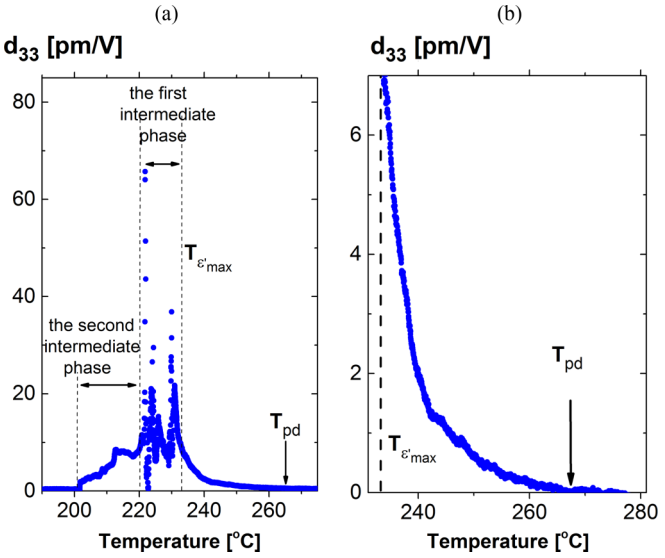

FIG. 7. (a) Piezoelectric coefficient d_{33} versus temperature for a $PbZrO_3$:Nb single crystal. (b) Temperature dependence of the piezoelectric coefficient d_{33} above $T_{\varepsilon'\max}$. T_{pd} is the temperature at which piezo activity vanishes.

On heating, the same description should be used, remembering that a thermal hysteresis of subsequent transitions has to be taken into account.

VII. CONCLUSIONS

It was possible to obtain a single crystal of lead zirconate doped with niobium with nominal value of 0.6 mol%, and of good quality. The room-temperature phase of this crystal is of macroscopic *Pbam* symmetry, like that in pure lead zirconate. It is interesting that within the antiferroelectric phase a complex domain structure appears, mostly with rounded domain boundaries. We guess that this is connected with an effect of clustering of unit cells containing Nb ions.

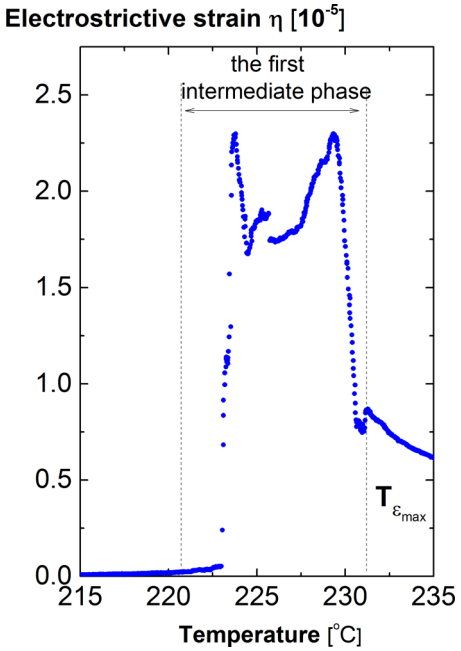

FIG. 8. Temperature changes of the electrostrictive strain $\eta \sim E^2$ for a $PbZrO_3$:Nb single crystal, on cooling.

Two intermediate phases were observed with the use of a few techniques measuring the dielectric, optical, and electromechanical properties. Both intermediate phases are of noncentrosymmetric symmetry, because under alternating electric field action, clear piezoelectric signals were detected. Moreover, the phase above T_C, in a wide temperature range, is not so simple as expected for an oxidic perovskite centrosymmetric paraelectric phase. According to the theory of Bussmann-Holder *et al.* [7], the crystal lattice in the paraelectric phase can be built of a centrosymmetric matrix with noncentrosymmetric local (polar) regions. The theoretical temperature limit of a lattice of this kind is calculated as $T_{BH} = 1.1\,T_C$, in fact not defining whether or not the noncentrosymmetric regions are persistent in the entire temperature region of $\langle T_C, T_{BH}\rangle$. In the case of $PbZrO_3$ slightly doped with Nb this question seems to be answered. Namely, above T_C there is the temperature T_{pd}, at which very stable and repeatable piezoelectric signals were observed, not depending on thermal cycles. On the other hand, near the same temperature, birefringence also disappears. The fact that we simultaneously observe the piezoelectric effect and birefringence means that in the region $\langle T_C, T_{pd}\rangle$ there are stable, persistent noncentrosymmetric regions which, under the action of a low-frequency alternating electric field, can vibrate, and through interaction with the matrix lead to macroscopic deformation of the piezoelectric character. On the other hand, these regions have to have locally deformed electronic structure, and interacting with light produces birefringence. Above T_{pd} inside the crystal lattice, there are still polar fluctuations; however, the thermal energy makes their correlation lengths too short to produce local stable distortions. It is consistent with recent reports on complex lattice instabilities above T_C [38–41], and also with the recent results of diffuse neutron scattering obtained for pure lead zirconate $PbZrO_3$, which showed (at 250 °C, i.e., just within the $\langle T_C, T_{pd}\rangle$ region) a disorder in the Pb sublattice and disorder in the tilts of oxygen octahedra [42]. Here, it is worth mentioning that the tilts of the octahedra are characteristic features of ferroelectric phases in $Pb(Zr,Ti)O_3$ solid solutions.

The question of an additional role of Nb, other than the influence on phase transitions or possible clustering of units containing Nb, should also be considered. We believe that for the concentration of Nb used, the dopant introduced to the lattice first of all enhances the charge neutrality, i.e., niobium may compensate for partial lead or oxygen vacancies. In effect it reduces the influence of point defect movements in the lattice, and hence the crystals under investigation were much more resistant to electric field actions. Due to that, it was possible to avoid electrochemical changes of the crystal surface, which often take place in ABO_3 perovskites (e.g., [43]).

ACKNOWLEDGMENTS

The authors are thankful for helpful remarks from A. M. Glazer and A. Leonarska.

[1] G. Shirane, E. Sawaguchi, and A. Takeda, Phys. Rev. **80**, 485 (1950).
[2] S. Roberts, J. Am. Ceram. Soc. **33**, 63 (1950).
[3] Y. Akiuama, S. Kimura, and I. Fujimura, Jpn. J. Appl. Phys. **32**, 4154 (1993).
[4] J. F. Li, D. D. Viehland, T. Tani, C. D. E. Lakeman, and D. A. Payne, J. Appl. Phys. **75**, 442 (1994).
[5] K. G. Brooks, J. Chen, K. R. Udayakumar, and L. E. Cross, J. Appl. Phys. **75**, 1699 (1994).
[6] V. J. Tennery, J. Electrochem. Soc. **112**, 1117 (1965).
[7] J.-H. Ko, M. Górny, A. Majchrowski, K. Roleder, and A. Bussmann-Holder, Phys. Rev. B **87**, 184110 (2013).
[8] V. J. Tennery, J. Am. Ceram. Soc. **49**, 483 (1966).
[9] L. Goulpeau, Sov. Phys. Solid State **8**, 1970 (1967).
[10] B. A. Scott and G. Burns, J. Am. Ceram. Soc. **55**, 331 (1972).
[11] Z. Ujma and J. Handerek, Phys. Stat. Solidi A **28**, 489 (1975).
[12] R. W. Whatmore and A. M. Glazer, J. Phys. C: Solid State Phys. **12**, 1505 (1979).
[13] Z. Ujma and J. Hańderek, Phase Transitions **3**, 121 (1983).
[14] Z. Ujma, Phase Transitions **4**, 169 (1984).
[15] Z. Ujma, D. Dmytrow, and J. Hańderek, Ferroelectrics **81**, 107 (1988).
[16] K. Wieczorek, Z. Ujma, K. Popek, I. Gruszka, M. Górny, J. Koperski, A. Soszyński, and K. Roleder, J. Phys.: Condens. Matter **21**, 115901 (2009).
[17] D. Viehland, Phys. Rev. B **52**, 778 (1995).
[18] B. Noheda, J. A. Gonzalo, L. E. Cross, R. Guo, S. E. Park, D. E. Cox, and G. Shirane, Phys. Rev. B **61**, 8687 (2000).
[19] S. Roberts, Phys. Rev. **83**, 1078 (1951).
[20] G. Shirane, Phys. Rev. **86**, 219 (1952).
[21] B. P. Pakharel and D. Pandy, J. Appl. Phys. **88**, 5364 (2000).
[22] L. Benguigui, J. Solid State Chem. **3**, 381 (1971).
[23] Z. Ujma, D. Dmytrow, and M. Pawełczyk, Ferroelectrics **120**, 211 (1991).
[24] Z. Ujma, H. Hassan, K. Wójcik, G. E. Kugel, and M. D. Fontana, Ferroelectrics **125**, 499 (1992).
[25] R. Rivera and A. Stashans, Phys. Scr. **78**, 045601 (2008).
[26] H. M. Rietveld, J. Appl. Crystallogr. **2**, 65 (1969)
[27] J. Rodriguez-Carvajal, Commission on Powder Diffraction (IUCr) Newsletter **26**, 12 (2001).
[28] M. A. Geday and A. M. Glazer, J. Phys.: Condens. Matter **16**, 3303 (2004)
[29] K. Wieczorek, A. Ziebińska, Z. Ujma, K. Szot, M. Górny, I. Franke, J. Koperski, A. Soszyński, and K. Roleder, Ferroelectrics **336**, 61 (2008).
[30] K. Yamasaki, Y. Soejimaa, and K. F. Fischer, Acta Crystallogr. B **54**, 524 (1998).
[31] P. Thompson, D. E. Cox, and J. B. Hastings, J. Appl. Crystallogr. **20**, 79 (1987).
[32] M. Jarvinen, J. Appl. Crystallogr. **26**, 527 (1993).
[33] P. W. Stephens, J. Appl. Crystallogr. **32**, 281 (1999).
[34] A. M. Glazer, K. Roleder, and J. Dec, Acta Crystallogr. B **49**, 846 (1993).
[35] A. Bussmann-Holder, J.-H. Ko, A. Majchrowski, M. Górny, and K. Roleder, J. Phys.: Condens. Matter **25**, 212202 (2013).
[36] C. Rodenbücher, W. Speier, G. Bihlmayer, U. Breuer, R. Waser, and K. Szot, New J. Phys. **15**, 103017 (2013).
[37] A. Ziębińska, D. Rytz, K. Szot, M. Górny, and K. Roleder, J. Phys.: Condens. Matter **20**, 142202 (2008).
[38] A. Bussmann-Holder, T. H. Kim, B. W. Lee, J.-H. Ko, A. Majchrowski, A. Soszyński, and K. Roleder, J. Phys.: Condens. Matter **27**, 105901 (2015).
[39] R. G. Burkovsky, D. Andronikova, Y. Bronwald, M. Krisch, K. Roleder, A. Majchrowski, A. V. Filimonov, A. I. Rudskoy, and S. B. Vakhrushev, J. Phys.: Condens. Matter **27**, 335901 (2015).
[40] A. Bussmann-Holder, K. Roleder, and J.-H. Ko, J. Phys.: Condens. Matter **26**, 275402 (2014).
[41] R. G. Burkovsky, A. K. Tagantsev, K. Vaideeswaran, N. Setter, S. B. Vakhrushev, A. V. Filimonov, A. Shaganov, D. Andronikova, A. I. Rudskoy, A. Q. R. Baron, H. Uchiyama, D. Chernyshov, Z. Ujma, K. Roleder, and A. Majchrowski, Phys. Rev. B **90**, 144301 (2014).
[42] N. Zhang, M. Paściak, M. A. Glazer, J. Hlinka, M. Gutmann, H. A. Sparkes, T. R. Welberry, A. Majchrowski, K. Roleder, Y. Xie, and Z.-G. Ye, J. Appl. Crystallogr. **48**, 1637 (2015).
[43] K. Roleder and J. Dec, J. Phys.: Condens. Matter **1**, 1503 (1989).